Accepted Manuscript

Revealing Halogen bonding Interactions with Anomeric Systems: An *ab initio* Quantum Chemical Studies

Rabindranath Lo and Bishwajit Ganguly*

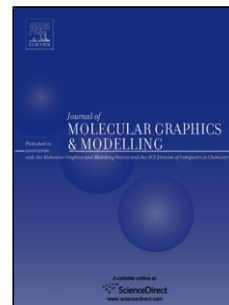*Computation and Simulation Unit (Analytical Discipline and Centralized Instrument Facility), CSIR-Central Salt & Marine Chemicals Research Institute, Bhavnagar, Gujarat, India-364 002*

Corresponding Author. Fax: (+91)-278-2567562, E-mail: *ganguly@csmcri.org*

Abstract: A computational study has been performed using MP2 and CCSD(T) methods on a series of $O \cdots X$ (X = Br, Cl and I) halogen bonds to evaluate the strength and characteristic of such highly directional noncovalent interactions. The study has been carried out on a series of dimeric complexes formed between interhalogen compounds (such as BrF, BrCl and BrI) and oxygen containing electron donor molecule. The existence and consequences of the anomeric effect of the electron donor molecule has also been investigated through an exploration of halogen bonding interactions in this halogen bonded complexes. The *ab initio* quantum chemical calculations have been employed to study both the nature and directionality of the halogen molecules towards the sp^3 oxygen atom in anomeric systems. The presence of anomeric $n_O \rightarrow \sigma^*_{C-N}$ interaction involves a dominant role for the availability of the axial and equatorial lone pairs of donor O atom to participate with interhalogen compounds in the halogen-bonded complexes. The energy difference between the axial and equatorial conformers with interhalogen compounds reaches up to 4.60 kJ/mol, which however depends upon the interacting halogen atoms and its attaching atoms. The energy decomposition analysis further suggests that the total halogen bond interaction energies are mainly contributed by the attractive electrostatic and dispersion components. The role of substituents attached with the halogen atoms has also been evaluated in this study. With the increase of halogen atom

1

size and the positive nature of σ-hole, the halogen atom interacted more with the electron donor atom and the electrostatic contribution to the total interaction energy enhances appreciably. Further, noncovalent interaction (NCI) studies have been carried out to locate the noncovalent halogen bonding interactions in real space.

Keywords: Halogen bonding; anomeric effect; interhalogen compounds; post-Hartee-Fock *ab initio* methods; energy decomposition analysis.

1. Introduction

Intermolecular halogen bonding interactions are highly directional [1] and exhibit applications in crystal engineering [2], materials chemistry [3], drug discovery [4] and solid state synthesis of organic molecules [5] in the field of supramolecular chemistry [6]. Such attractive interactions occur from the terminal positive electrostatic potential (ESP), known as σ-hole, of covalently bound halogens along the direction of the R-X bonds [7]. Halogen bonds can be considered as short range R-X··YZ type of interaction, where X is a halogen (typically chlorine, bromine, or iodine) that is part of the molecule RX and YZ is a Lewis base (where Y is typically oxygen, nitrogen, or sulfur). The strength of the R-X··YZ halogen bond is related to the group adjacent with X. This noncovalent interaction is enhanced when the X atom is joined with an electron-withdrawing atom or group and Y atom is connected with an electron-donating atom or group. The electron-withdrawing nature of the substituent group (R) enhances the magnitude of $V_{S,max}$ (the most positive electrostatic potential at the σ-hole). Halogen bonding may occur with dihalogens X_2[7f] and interhalogens X-Y as well as organic halides. The interhalogen compounds with higher polarizability demonstrate the significant interactions energies with respect to a specific donor molecule.

2

In this study, second-order Møller-Plesset perturbation theory (MP2) calculations and coupled cluster method including singles, doubles and triples term (CCSD(T)) were employed on a series of O⋯X halogen bonds between O-containing donor molecule and Br-containing interhalogen compounds. The possibility of the formation of halogen bonding has also been examined through both sides of the interhalogen compounds (FBr, ClBr and IBr) with a given donor molecule. In earlier reports, most of the halogen bonding interactions has been shown by the involvement of halogen compounds and carbonyl oxygen [8]. The earlier database survey implies that 78 out of 113 X…O halogen bonding interactions engaged with carbonyl groups [9]. Numerous theoretical calculations are performed to characterize the geometric and energetic properties of X…O halogen bonds involving sp^2 and sp^3 oxygen donor atoms [10]. Further, evidences of such type of interactions are achieved through a broad range of molecular complexes and crystals [11]. Herein, we have considered tetrahydro-1,3-oxazine as oxygen containing electron donor molecule in this study. The stereoelectronic effects have been observed due to the presence of axial and equatorial lone pairs of oxygen atom in this cyclic electron donor molecule, which assists to perform a detailed analysis of halogen bonding interactions in this anomeric system. Furthermore, this cyclic system is rigid and hence can segregate the difference between the axial and equatorial oxygen lone-pairs. The stereoelectronic behavior of X-C-Y containing systems (X, Y = OR, NR$_2$, Hal), known as the anomeric effect, has been widely studied in the literature [12]. Generally, the magnitude of anomeric effect is only a few kcal/mol and thus comparable to the strength of conventional hydrogen bonds [12]. The anomeric effect refers to the thermodynamic preference of glycopyranosyl derivatives with electronegative (polar) substituents adjacent to the endocyclic oxygen atom in an axial position (α anomer) rather than an equatorial position (β anomer) in the chair conformation [12]. In many chemical reactions and carbohydrate chemistry, the anomeric effect ubiquitously exists. It is widely assumed that both steric and electronic interactions create contributions to the conformational preferences, although their exact roles are controversial. Currently, the popular explanation for the anomeric effect is

3

hyperconjugation model [13], where the electron delocalization occur from the lone pair of electron donor atom to the vacant antibonding orbital σ^*_{C-Y} (Scheme 1). As a result, various structural parameters are found to be changed e.g., shorter or longer anomeric bonds and larger anomeric bond angles. Another explanation for the anomeric effect is the electrostatic model [14], which was originally from antiparallel arrangement of the two local dipoles in the axial conformer stabilizes the molecule (Scheme 1).
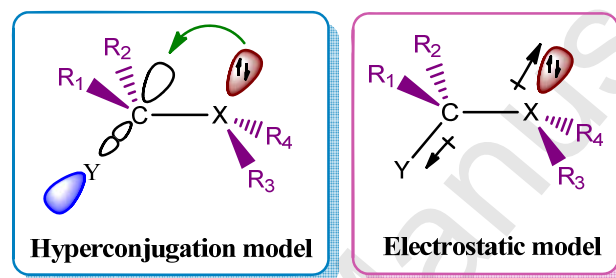
Scheme 1: Schematic representation of Hyperconjugation and electrostatic model.

In this article, we have examined halogen bonding interactions of C-O···X-R type with anomeric system tetrahydro-1,3-oxazine and interhalogen compounds. Tetrahydro-1,3-oxazines can be regarded as unsymmetrical 1,3-heteroanalogs of cyclohexane. The heteroatom lone pairs in such systems are stereoelectronically different and hence the approach of interhalogen compounds would be differentiated towards such lone pairs (Scheme 2). The energetic difference between these halogenated complexes indicates the influence of the stereoelctronic effect in these cases. Therefore, the directionality of the interhalogen compounds towards the oxygen atom would be governed by the stereoelectronic effects. The importance of directionality is highly desirable in crystal engineering and supramolecular assembly for the development of new materials.

4
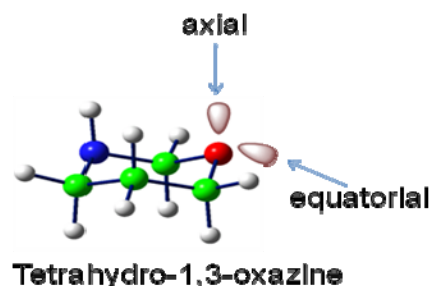
Scheme 2: Axial and equatorial lone pair sides of tetrahydro-1,3-oxazine.

2. Computational Details

The geometry of organic molecule and its complexes with BrF, BrCl, BrI molecules were fully optimized at MP2/aug-cc-pVDZ [15] level of theory with Gaussian 09 [16]. LANL2DZ basis set was used for iodine in this study. The level of theory adopted in this study has been reported to show good correlation with the standard CCSD(T) with larger basis sets as well as with the available experimental quantities for various weak intermolecular interactions [17]. The harmonic vibrational frequency calculations were used to confirm that the optimized structures were minima, as characterized by positive vibrational frequencies. The interaction energy for the intermolecular O···X interactions was calculated using the following equation:

$$E_{(\text{interaction energy})} = E_{(\text{complex})} - E_{(\text{molecule 1})} - E_{(\text{molecule 2})} \cdots\cdots (1)$$

This eq. 1 has been computed in two different approaches. In this first approach, we have taken the optimized geometries of the monomers, however, in second approach we have taken monomer geometries from the optimized complexes without any further structural changes. The calculated interaction energies were also corrected by the basis set superposition error (BSSE). The standard counterpoise procedure of Boys and Bernardi was used for single point BSSE correction at MP2/aug-cc-pVDZ level of theory without further optimization of the geometries [18]. Single point calculations were performed at CCSD(T)/aug-cc-pVDZ level of theory with the optimized complex geometries. The electrostatic

5

potentials were computed with Multiwfn program [19] on the 0.001 au surface of the molecules electron density [20]. Subsequently, the noncovalent interaction (NCI) index calculations were also performed with Multiwfn program [19] and visualized using the VMD program [21]. The atoms in molecules (AIM) calculations using Bader's [22] AIM theory were performed with the wave functions generated from the MP2/aug-cc-pVDZ level of theory in AIM2000 software [23]. Some bond paths, which are not generated in AIM2000 software, are calculated from Multiwfn program and shown in the Figs. with dotted line. NBO analysis was performed from NBO 3.1 program [24] as implemented in Gaussian 09 using the optimized geometries.

3. Results and Discussion

Molecular electrostatic potentials, Geometries and halogen-bonded interaction energies

The molecular electrostatic isopotential surfaces (MESP) of the interhalogen compounds are computed and presented in Fig. 1. The molecular electrostatic isopotential surface (MESP) provides an effective tool for quantitatively measuring various noncovalent interactions, such as hydrogen bonding and cation-π interactions [25]. The electropositive regions (σ-hole) are present on the outer surface of the X (X= Cl, Br, I) atom along the extension of the R-X bond. The presence of electron-withdrawing substituent can enhance the size of the σ-hole. For a given halogen atom (Br), the $V_{S,max}$value decreases in the consequence of decreasing electron withdrawing nature of R (F>Cl>I) (Fig. 1). The most positive electrostatic potentials of the σ-hole are found to be associated with bromine atom of FBr. Further, it is observed that $V_{S,max}$value correlates with the halogen polarizibility (mass number of the atom). In the presence of same substituent groups $V_{S,max}$value follows the order Cl < I (Fig. 1). The most electronegative F atom does not contain any positive electrostatic potential value to interact with the electron-donor atoms (Fig. 1). However, F atom in BrF is characterized by negative electrostatic potential

6

value and thus can act as Lewis base center. Therefore, we have examined the halogen bonding complexes of donor molecule with Cl, Br and I centers of interhalogen compounds.
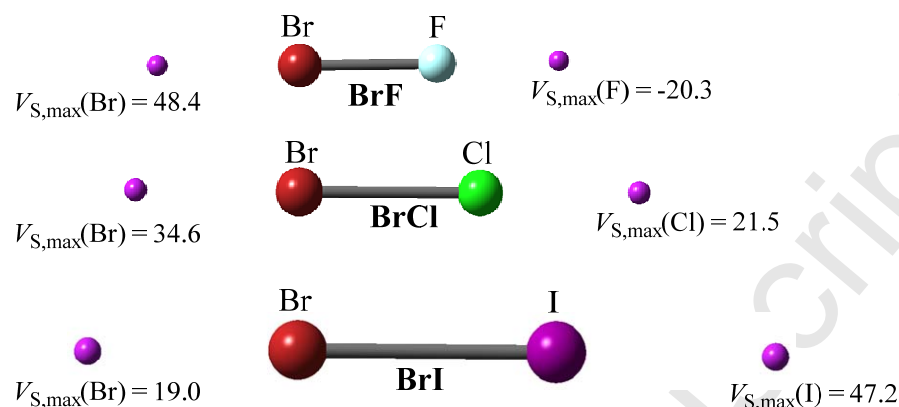

Fig. 1: The maximum electrostatic potential ($V_{S,max}$, kcal/mol) of halogen atom for BrF, BrCl and BrI molecules.[dark red = bromine; cyan = fluorine; dark violet = chlorine; indigo = iodine]

The possible geometric arrangements (axial and equatorial approach) of tetrahydro-1,3-oxazine with interhalogen complexes have been optimized (Fig. 2). The interaction of interhalogen compounds with the axial and equatorial lone-pairs of tetrahydro-1,3-oxazine has been studied. The un-substituted tetrahydro-1,3-oxazine was reported to exist mainly as *chair* conformer with the axial N–H bond [26]. Therefore, we have also chosen the *chair* conformer of tetrahydro-1,3-oxazine with axial N–H bond for the complexation of interhalogen compounds.

The approach of R-X molecule towards the axial and equatorial lone-pairs of donor oxygen of tetrahydro-1,3-oxazine was optimized in all cases. The converged complexes for the interactions of tetrahydro-1,3-oxazine with FBr, ClBr and IBr were all minimum (Fig. 2). In such structures, the O…Br intermolecular distances is substantially shorter than the sum of the van der Waals radii of the O and Br atoms (O, 1.50 Å; Br, 1.85 Å) (Fig. 2) [27]. In the case of FBr, the calculated O…Br-F angle is approximately 180º, which indicates that the halogen bonding is highly directional (Fig. 2) [1]. The

7

calculated O…Br non-bonded distance for 1_{eq} is found to be 2.305 Å, whereas in 1_{ax} similar bond distance occurs (Fig. 2). The interaction energy calculated for 1_{eq} complex at CCSD(T) level is -13.8 kcal/mol, which is energetically higher than the computed O…Br interaction energy for 1_{ax} (-14.4 kcal/mol) (Table 1). These calculated results indicate that the bromine atom of FBr can interact preferentially with the axial lone-pair of donor oxygen in tetrahydro-1,3-oxazine than the equatorial lone-pair. This might be attributed due to the anomeric effect of parent tetrahydro-1,3-oxazine molecule. From NBO analysis, it has been seen that there is a greater delocalization interaction occur between the equatorial lone pair of oxygen atom and C-N antibonding orbital ($n_{Oeq} \rightarrow \sigma^*_{C-N}$) compared to axial lone pair ($n_{Oax} \rightarrow \sigma^*_{C-N}$). Importantly, greater second-order perturbation stabilizing energy is found in $n_{Oeq} \rightarrow \sigma^*_{C-N}$ interaction (11.5 kcal/mol) than $n_{Oax} \rightarrow \sigma^*_{C-N}$ interaction (1.5 kcal/mol) at MP2/aug-cc-pVDZ level of theory. Hence, the greater involvement of equatorial lone pair in hyperconjugative interaction with antiperiplanar C-N σ* orbital stabilizes the system and consequently it should be less available for the complexation with the FBr molecule.

The interaction of tetrahydro-1,3-oxazine with BrCl molecule also provides similar type of geometries as we obtained with BrF molecule in tetrahydro-1,3-oxazine:BrF system. The calculated O…Br distances and O…Br-Cl angles for axial and equatorial interactions were found to be very similar in both cases (Fig. 2). The interaction energies for the tetrahydro-1,3-oxazine:BrCl complexes showed that the attraction between tetrahydro-1,3-oxazine and BrCl in axial position is higher compared to the equatorial position at CCSD(T)/aug-cc-pVDZ level of theory (Table 1).

The stereoelectronic effects have also been observed in tetrahydro-1,3-oxazine and BrI complexes due to the involvement of axial and equatorial lone pairs of oxygen atoms in tetrahydro-1,3-oxazine. Two different geometries were obtained for tetrahydro-1,3-oxazine with BrI molecule with MP2/aug-cc-pVDZ level of theory (Fig. 2). The computed geometrical parameters show that the O⋯Br-I bond angle in

8

3_{ax} tends to be more collinear (178.1º) than corresponding bond angle in 3_{eq} (175.6º) (Fig. 2). Furthermore, there is slight deviations observed in the structural parameters between axial and equatorial complexes of tetrahydro-1,3-oxazine with BrI (Fig. 2). The preferential binding of BrI towards axial position of donor oxygen is also observed compared to the equatorial position (Table 1).

1_{eq}: Tetrahydro-1,3-oxazine: BrF **1_{ax}: Tetrahydro-1,3-oxazine: BrF**

2_{eq}: Tetrahydro-1,3-oxazine: BrCl **2_{ax}: Tetrahydro-1,3-oxazine: BrCl**

3_{eq}: Tetrahydro-1,3-oxazine: BrI **3_{ax}: Tetrahydro-1,3-oxazine: BrI**
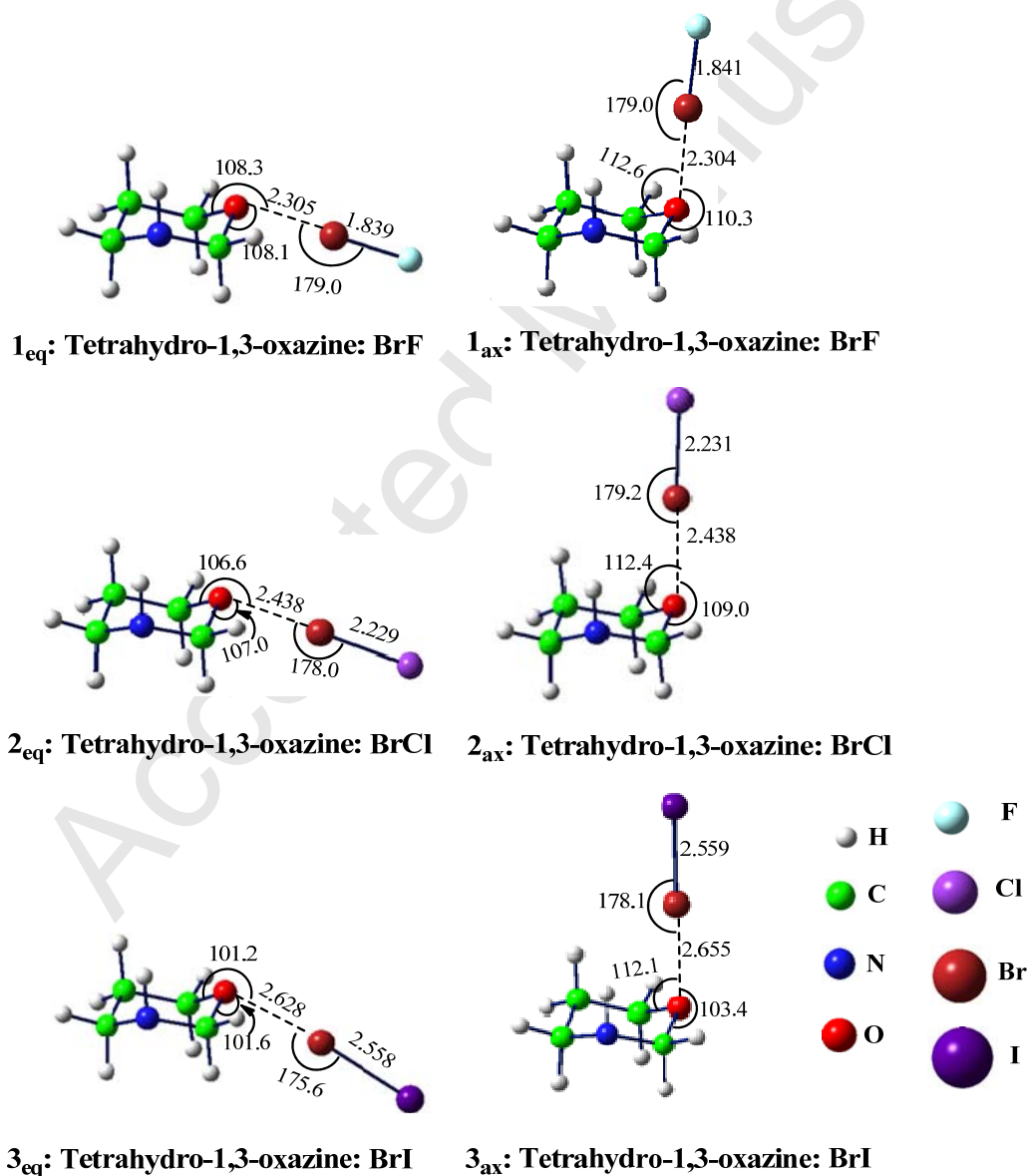
9

Fig. 2: MP2/aug-cc-pVDZ optimized geometries for tetrahydro-1,3-oxazine with BrF, BrCl and BrI. (LANL2DZ basis set is used for iodine) [Distances are in Å and angles are in degrees] [Green = carbon; white = hydrogen; red = oxygen; dark blue = nitrogen; dark red = bromine; cyan = fluorine; dark violet = chlorine; indigo = iodine]

Table 1: The calculated binding energies of the halogen-bonded complexes are in kcal/mol. In parenthesis, the binding energies are calculated in which it is assumed that in complex geometry there is no structural change of monomers.

	MP2/aug-cc-pVDZ	CCSD(T)/aug-cc-pVDZ //MP2/aug-cc-pVDZ
	BSSE corrected	
1. X=F		
1_{eq}	-11.5 (-12.7)	-13.8
1_{ax}	-11.8 (-13.2)	-14.4
2. X=Cl		
2_{eq}	-7.4 (-8.2)	-10.1
2_{ax}	-7.8 (-8.7)	-10.8
3. X=I		
3_{eq}	-3.4 (-3.5)	-8.7
3_{ax}	-4.0 (-4.1)	-9.7

We have examined the halogen bonded interactions of tetrahydro-1,3-oxazine towards Br atom of interhalogen compounds. Furthermore, the study has been extended for halogen-bonded interaction with tetrahydro-1,3-oxazine and other atomic sites of interhalogen compounds. For FBr, there is no electropositive region present in fluorine atom, hence we have examined the halogen bonding interactions with only Cl and I centers of interhalogen compounds. The optimized geometries predicted for tetrahydro-1,3-oxazine with ClBr and IBr molecules are given in Fig. 3. The computed O⋯Cl-Br bond angle of tetrahydro-1,3-oxazine:ClBr was found to be slightly larger in axial cases (178.2º) compared to the equatorial approach (175.5º) (Fig. 3). The interaction energies for the tetrahydro-1,3-oxazine:ClBr

10

complexes showed that the attraction between tetrahydro-1,3-oxazine and ClBr in axial position is higher compared to the equatorial position (Table 2). The calculated interaction energies suggest that the O atom of tetrahydro-1,3-oxazine is interacted more strongly with the Br atom of BrCl than the Cl atom due to the presence of higher $V_{S,max}$ value in bromine center (34.6 kcal/mol) compared to that of Cl (21.5 kcal/mol) (Tables 1-2 and Fig. 1). The preferences for the axial interaction over equatorial interaction for tetrahydro-1,3-oxazine with BrCl is similar for both sites of the interhalogen compound.

The calculated geometrical parameters show small deviations in axial and equatorial complexes with IBr (Fig. 3). The preferential binding of IBr towards axial position of donor oxygen is also observed compared to the equatorial position. The axial geometry ($3'_{ax}$) is energetically stable than corresponding equatorial geometry ($3'_{eq}$) by 1.1 kcal/mol in tetrahydro-1,3-oxazine:IBr complex (Fig. 3, Table 2).
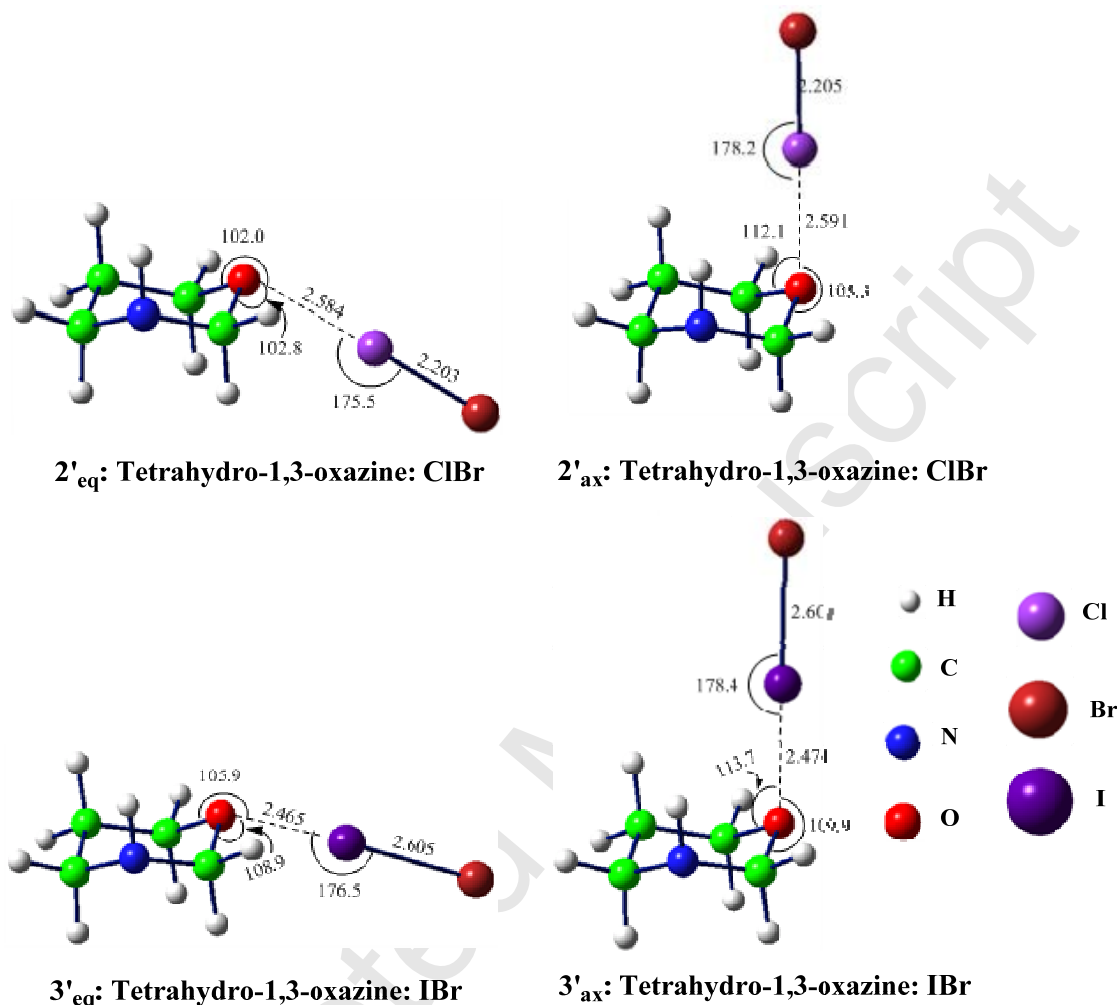
11

2'eq: Tetrahydro-1,3-oxazine: ClBr

2'ax: Tetrahydro-1,3-oxazine: ClBr

3'eq: Tetrahydro-1,3-oxazine: IBr

3'ax: Tetrahydro-1,3-oxazine: IBr

Fig. 3: MP2/aug-cc-pVDZ optimized geometries for tetrahydro-1,3-oxazine with ClBr and IBr. (LANL2DZ basis set is used for iodine) [Distances are in Å and angles are in degrees] [Green = carbon; white = hydrogen; red = oxygen; dark blue = nitrogen; dark red = bromine; cyan = fluorine; dark violet = chlorine; indigo = iodine]

Table 2: The calculated binding energies of the halogen-bonded complexes are in kcal/mol. In parenthesis, the binding energies are calculated in which it is assumed that in complex geometry there is no structural change of monomers.

12

	MP2/aug-cc-pVDZ	CCSD(T)/aug-cc-pVDZ //MP2/aug-cc-pVDZ
	BSSE corrected	
2′. X=Cl		
2′$_{eq}$	-3.9 (-4.1)	-5.8
2′$_{ax}$	-4.4 (-4.6)	-6.4
3′. X=I		
3′$_{eq}$	-6.6 (-7.7)	-14.1
3′$_{ax}$	-7.0 (-8.2)	-15.2

Decomposition of binding energies

To get a better insight on the nature of halogen bonding with anomeric oxygen atoms, it is important to decompose the noncovalent halogen-bonded interaction into various ''components'' and to quantify their contributions to the binding energy. Various procedures have been introduced for partitioning the binding energy into different subsets like electrostatics, dispersion, charge transfer, polarization, exchange repulsion, induction, orbital interaction, Pauli repulsion and distortion, etc [28]. In this study, we have utilized localized molecular orbital energy decomposition analysis (LMO-EDA) for energy decomposition analysis [29]. LMO-EDA method as implemented in the GAMESS software is carried out to examine the factors contributing to such interaction energies [30]. LMO-EDA method offers to fragment the total interaction energy (ΔE_{int}) into electrostatic (ΔE_{ele}), exchange (ΔE_{ex}), repulsion (ΔE_{rep}), polarization (ΔE_{pol}) and dispersion (ΔE_{disp}) components [28].

$$\Delta E_{int} = \Delta E_{ele} + \Delta E_{ex} + \Delta E_{rep} + \Delta E_{pol} + \Delta E_{disp}$$

The earlier studies have demonstrated that the halogen bonds are stabilized primarily by electrostatics and dispersion contribution [31]. Several halogen bonding and other σ-hole interactions are adequately and fully explained by electrostatics/polarization and dispersion as the principle attractive components [31].The calculated results show that the stabilities of the O··Br and O··Cl halogen bonds are attributed mainly to electrostatic and dispersion forces (Table 3). The attractive "dispersion" term computed in the

13

LMO-EDA method arises due to the presence of electron correlation in the system [28].The greater electrostatic values indicate the better orbital overlapping between electron donor and interhalogen compounds. Further, the large exchange and repulsion terms also implies the feasibility of orbital overlapping between the two monomers. The exchange energy obtained from LMO-EDA analysis is similar to the charge transfer term in NEDA or Morokuma partitioning scheme [32]. The polarization terms are also attractive in nature in these interhalogen complexes and such effects are considered by the orbital interactions between monomers which further allows charge shift between the respective monomers [28b]. The polarization effects in axial interactions are considerably larger than the equatorial one, which further contributes to the total interaction energies (Table 3).The total interaction energies calculated in LMO-EDA method are similar to the BSSE corrected interaction energies calculated with Gaussian 09 program (Tables 1-3). In the presence of electron-withdrawing substituents, the halogen bonding interactions become stronger and more electrostatic in nature. The LMO-EDA analysis suggests that the electrostatic forces in tetrahydro-1,3-oxazine:BrF complexes are larger than other interhalogen complexes (Table 3). Further, the larger size of the halogen atom influences to increase the strength of the halogen bonding interaction by enhancing the electrostatic forces in the halogen bonded complexes (Table 3).

Table 3: LMO-EDA decomposed energy terms in kcal/mol at MP2/aug-cc-pVDZ level of theory.

	1_{eq}	1_{ax}	2_{eq}	2_{ax}	$2'_{eq}$	$2'_{ax}$
Electrostatic	-31.45	-33.28	-21.84	-23.44	-9.60	-10.68
Exchange	-46.36	-50.04	-36.45	-39.87	-19.10	-21.30
Repulsion	89.56	96.27	68.22	74.31	34.23	38.08
Polarization	-17.73	-18.61	-10.78	-11.44	-4.11	-4.45
Dispersion	-6.78	-7.60	-7.35	-8.31	-5.55	-6.30
Total	**-12.76**	**-13.26**	**-8.21**	**-8.76**	**-4.13**	**-4.65**

Topological Analysis

14

Bader's quantum theory of "atoms in molecules" (QTAIM) has been widely used to characterize halogen and hydrogen bonds in a precise way [33]. The local topological properties of the electron density are estimated in the studied halogen bonds to get a thorough insight of these interactions. In QTAIM, the value of electron density, ρ indicates the strength of the non-covalent interactions. The sign of the Laplacian of the density, $\nabla^2\rho$, is mainly used to distinguish between different types of strong interactions [34]. The molecular graphs of the halogen bonded complexes are plotted in Figs. 4 and 5. The calculated electron densities as well as its Laplacian have almost similar values in both equatorial and axial halogen bonded complexes (Table 4). However, in axial halogen bonded complexes, second bond critical point is found as a result of Br/X···HC interaction (Figs. 4 and 5). In some cases, NH proton also participates in the hydrogen bonding with the electronegative halogen atoms. Such secondary interaction also contributed to stabilize the axial halogen bonded geometry along with the stereo-electronic effect.

Table 4: The topological parameters at the O…Br BCPs of the complexes in MP2/aug-cc-pVDZ level of theory.

	$\rho(r_c)$	$\nabla^2_{\rho(r_c)}$		$\rho(r_c)$	$\nabla^2_{\rho(r_c)}$
1_{eq}	0.0483	0.1604	$2'_{eq}$	0.0247	0.0962
1_{ax}	0.0483	0.1601	$2'_{ax}$	0.0241	0.0944
2_{eq}	0.0375	0.1294	$3'_{eq}$	0.0422	0.1136
2_{ax}	0.0374	0.1290	$3'_{ax}$	0.0411	0.1122
3_{eq}	0.0264	0.0934			
3_{ax}	0.0248	0.0882			

15

1_eq: Tetrahydro-1,3-oxazine: BrF   **1_ax: Tetrahydro-1,3-oxazine: BrF**

2_eq: Tetrahydro-1,3-oxazine: BrCl   **2_ax: Tetrahydro-1,3-oxazine: BrCl**

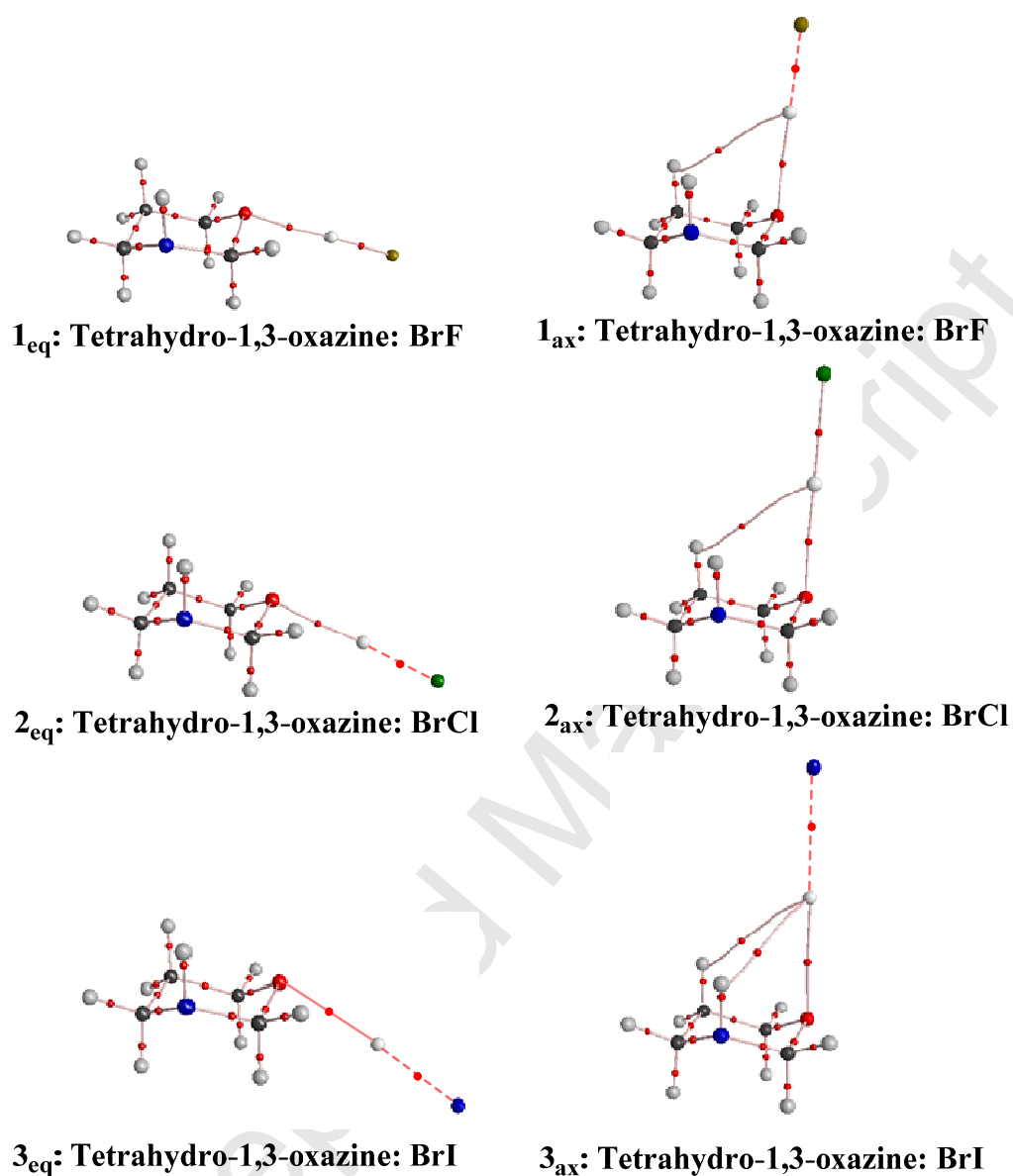**3_eq: Tetrahydro-1,3-oxazine: BrI**   **3_ax: Tetrahydro-1,3-oxazine: BrI**

Fig. 4: Molecular graphs of halogen-bonded complexes for tetrahydro-1,3-oxazine with interhalogen compounds (BrF, BrCl and BrI). Small red dots indicate critical points.
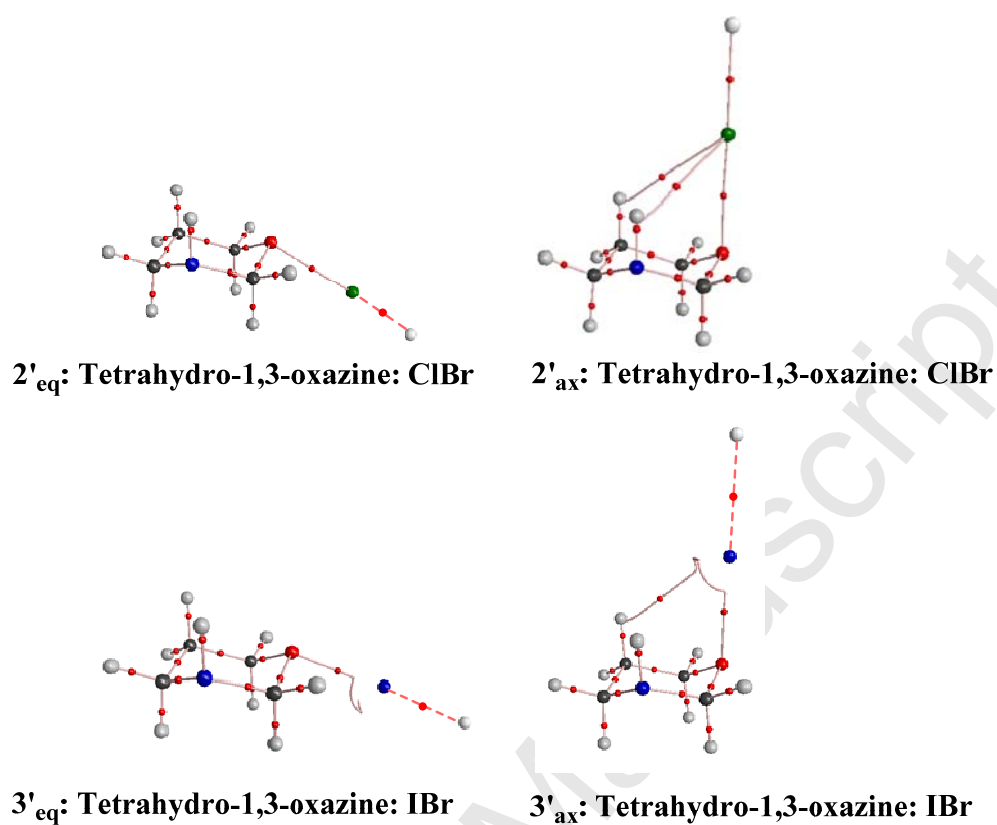
16

2'$_{eq}$: Tetrahydro-1,3-oxazine: ClBr   **2'$_{ax}$: Tetrahydro-1,3-oxazine: ClBr**

3'$_{eq}$: Tetrahydro-1,3-oxazine: IBr   **3'$_{ax}$: Tetrahydro-1,3-oxazine: IBr**

Fig. 5: Molecular graphsof halogen-bonded complexes for tetrahydro-1,3-oxazine with interhalogen compounds (ClBr and IBr). Small red dots indicate critical points.

17

The contour maps of Laplacian of the electron density for the halogen bonded complexes are generated in Fig. S1. All the maps contain a plane of C, Br and X atoms. The bond paths and interatomic surfaces are generated by the gradient vector field of $\rho(r_c)$ and included in the maps. There is charge concentration in the valence-shell of the interacting halogen atom found above and below of the inter-nuclear axis (Fig. S1). Such results further suggest the existence of electropositive character along the internuclear axis. Alternatively, the nucleophilic character exist perpendicular to the axis. The region of negative values of Laplacian of the electron density ($\nabla^2 \rho_{(r)}$) implies the charge concentration

space, whereas the charge depletion occur in the region of positive value. In axial halogen bonded complexes, the O…Br bond critical point specify the halogen bond interaction and there is a second BCP found in Br$^{...}$H-C bond paths. The nucleophilic character of Br atom is responsible for such hydrogen bonding in these geometries.

**Noncovalent Interactions (NCI) index of the halogen bond**

The noncovalent interaction (NCI) index is based on the relationship between the electron density and the reduced density gradient [35]. Such approach has been taken in recent times to detect noncovalent interactions in real space, based on the electron density and its derivatives. This analysis provides a rich representation of van der Waals interactions, hydrogen bonds, and steric repulsion in small molecules, molecular complexes, and solids.
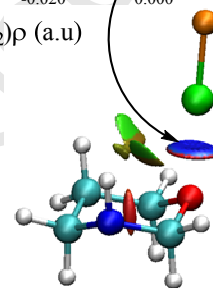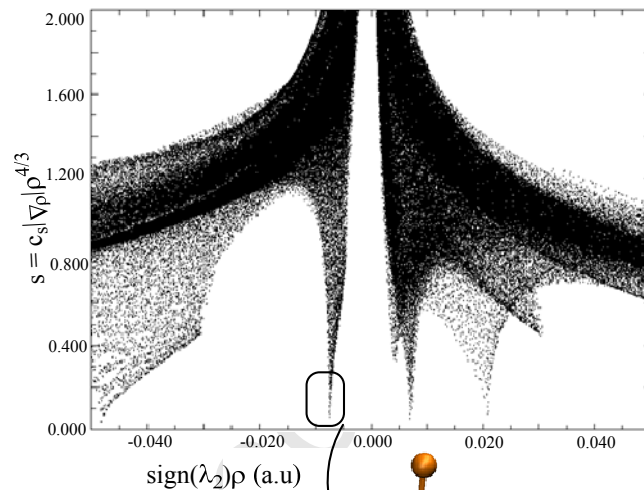
The reduced density gradient is expressed as,

$$s = \frac{1}{2(3\pi^2)^{1/3}} \frac{|\nabla \rho|}{\rho^{4/3}}$$

The reduced density gradient can be useful to identify the noncovalent interactions and covalent interactions in real space. Therefore, the NCI index becomes valuable tool to distinguish and visualize

different types of noncovalent interactions in real space. For better understanding the bonding, the Laplacian is often decomposed into a sum of contributions along the three principal axes of maximal variation, such that $\nabla^2_\rho = \lambda_1 + \lambda_2 + \lambda_3$. The analysis of these components has been widely applied to chemical bonding. ρ and $sign(\lambda_2)$, the sign of λ_2 are accomplished of distinguishing the type and strength of the interactions. Therefore, it is considered that large value of ρ and negative sign of $sign(\lambda_2)$ indicates the attractive interaction, whereas large value of ρ and positive sign of $sign(\lambda_2)$ suggest that the interaction is nonbonding [35]. Fig. 6 and Fig. S2 show the $s(\rho)$ vs $sign(\lambda_2)\rho$ in the halogen-bonded complexes with the low density, low-gradient spike lying at negative values indicative of stabilizing interactions of halogen bonding. In 1_{ax}, the spike is deviated more from zero compared to 1_{eq} and it becomes consistent with the trend of interaction energy of these halogen complexes. In the internuclear region between halogen atom and donor oxygen atom of the halogen-bonded complexes, there is a presence of bonding isosurface (Fig. 6). The color code of these bonding isosurfaces is from blue to green, which indicates that the halogen bond interactions are becoming weaker in the sequence of tetrahydro-1,3-oxazine:BrF, tetrahydro-1,3-oxazine:BrCl, tetrahydro-1,3-oxazine:BrI (Fig. 6).
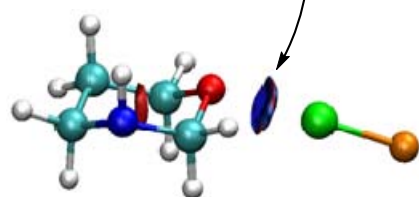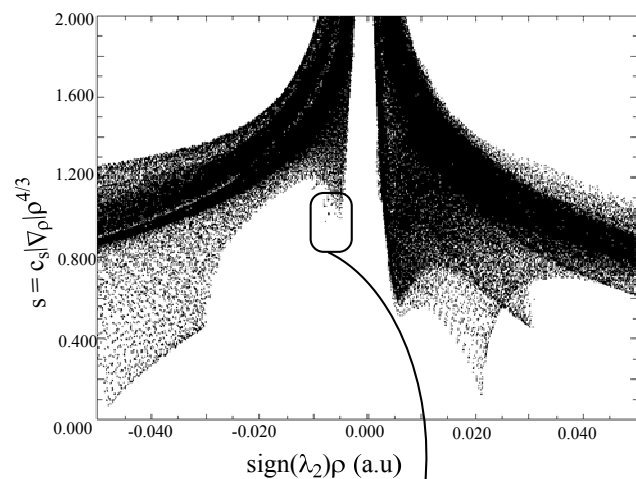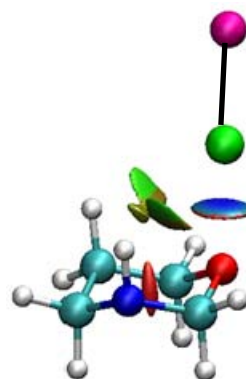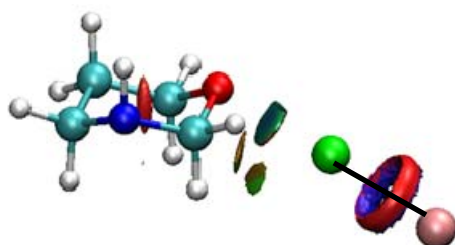
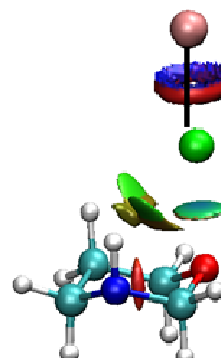**1_{eq}: Tetrahydro-1,3-oxazine: BrF**
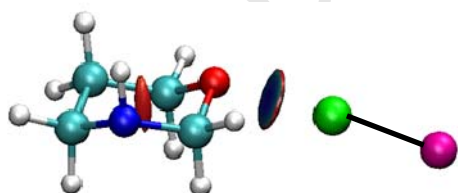
1_{ax}: Tetrahydro-1,3-oxazine: BrF

2_{eq}: Tetrahydro-1,3-oxazine: BrCl

2_{ax}: Tetrahydro-1,3-oxazine: BrCl

3_{eq}: Tetrahydro-1,3-oxazine: BrI

3_{ax}: Tetrahydro-1,3-oxazine: BrI

$\rho > 0$
$\lambda_2 < 0$

$\rho \sim 0$
$\lambda_2 \sim 0$

$\rho > 0$
$\lambda_2 > 0$

Strong attraction:
H-bond, Halogen-bond

Van der Waals
interaction
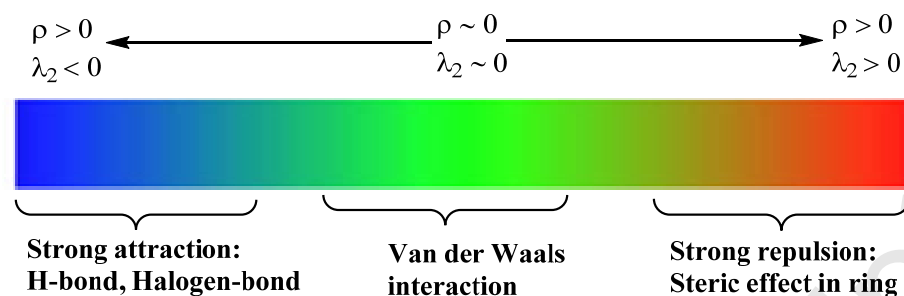
Strong repulsion:
Steric effect in ring

Fig. 6: Plots of the reduced density gradient versus the electron density multiplied by the sign of the second Hessian eigen value and bonding isosurfaces were generated.

To have a further insight into the halogen bonding, the changes in electron density that arises during the formation of the complexes were analysed. Total electron density maps have been shown to accurately determine electron density shifts [36]. The electron density shifts that occur in tetrahydro-1,3-oxazine:BrF complexes are shown in Fig. 7. These maps were generated by subtracting the sum of the electron densities of the isolated subsystems frozen in the optimized structure of the complex from the electron density in the complex. Red regions indicate increased electron density, whereas dark blue regions represent decreased electron density. Increased electron density is observed at the inter-nuclear position of the halogen-bonded complexes (Fig. 7). In 1_{ax} complex, there is a large decrease of blue region in the σ-hole on the Br atom of BrF compared to 1_{eq} complex, which suggests the greater charge transfer in the internuclear space (Fig. 7).

1_{eq}: Tetrahydro-1,3-oxazine: BrF   **1_{ax}: Tetrahydro-1,3-oxazine: BrF**
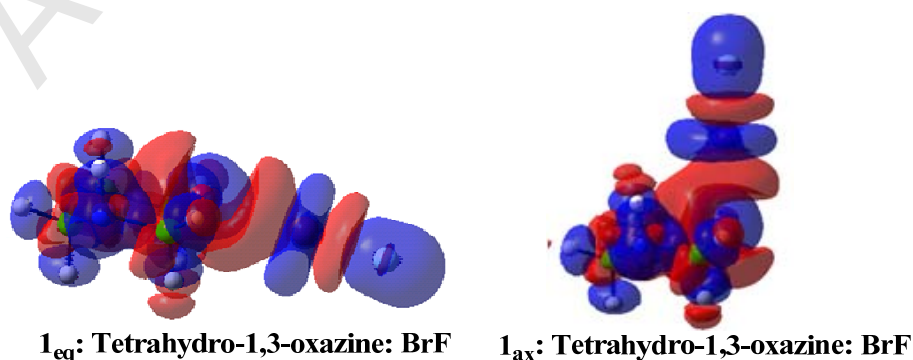
Fig. 7: Electron density shifts in the Halogen-bonded complexes upon the formation of each complex. Red regions indicate increased density, dark blue regions indicate decreased density. Contours are shown at the 0.001 au level.

Natural Bond Orbitals (NBO) analysis

The electron density shifts in the halogen-bonded complexes can also be described by NBO analysis [37]. Such procedure provides the role of intermolecular orbital interactions by examining the charge transfer, the second-order perturbation energy $E(2)$ (donor$\rightarrow$ acceptor). The NBO analyses were performed with the optimized geometries at the MP2/aug-cc-pVDZ level of theory. The occupancy in the lone pair orbital of donor molecule and the antibonding orbital of the interhalogen compounds has been evaluated before and after the complex formation. The calculated results show that there is considerable changes occur in the occupation number for the halogen bonded complexes. The occupancy in the lone pair orbital of donor molecule decreases notably in both axial and equatorial interactions compared to the ideal occupation number (Table 5). In equatorial interaction, large decrease in occupation number is found in halogen bonded complexes. The strong intra- and intermolecular charge transfer from the lone pair of O atom ($n_O \rightarrow \sigma^*_{Br-X}$ and $n_O \rightarrow \sigma^*_{C-N}$ supports the lower occupation number in equatorial interaction. These calculated results indicate the lower availability of equatorial lone pair for the interaction of interhalogen molecules. The calculated second-order perturbation energies also favor the axial interactions in most of the cases (Table 5). Moreover, there is considerable increase in occupation number of σ^*_{Br-} or σ^*_{X-i} anti bonding orbital in axial interaction, which implies stronger charge transfer interactions in axial direction than equatorial one (Table 5).

Table 5: Natural bond orbital analysis at the MP2/aug-cc-pVDZ level: the Second-Order Perturbation Energies $E(2)$ involving $n_O \to \sigma^*_{Br-}$ and $n_O \to \sigma^*_{C-}$; occupation number (e) for the n_O lone pairs and σ^*_{Br-} and σ^*_{X-} antibonds.

| | $E(2)$ (kcal/mol) | | | | | |
	$n_O \to \sigma^*_{Br-X}$	$n_O \to \sigma^*_{C-N}$	n_O	Δn_O^{a}	σ^*_{Br-X}	$\Delta \sigma^*_{Br-}{}^{b}$
1$_{eq}$	37.31	7.61	1.875	0.065	0.090	0.090
1$_{ax}$	38.15	7.40	1.878	0.062	0.096	0.095
2$_{eq}$	21.20	9.03	1.899	0.041	0.061	0.061
2$_{ax}$	21.69	6.87	1.902	0.038	0.066	0.066
3$_{eq}$	9.04	10.72	1.919	0.021	0.033	0.033
3$_{ax}$	8.38	5.70	1.924	0.016	0.036	0.036

| | $E(2)$ (kcal/mol) | | | | | |
	$n_O \to \sigma^*_{X-Br}$	$n_O \to \sigma^*_{C-N}$	n_O	Δn_O^{a}	σ^*_{X-Br}	$\Delta \sigma^*_{X-}{}^{b}$
2′$_{eq}$	6.68	11.03	1.925	0.016	0.025	0.025
2′$_{ax}$	6.27	6.68	1.929	0.012	0.028	0.028
3′$_{eq}$	33.95	7.75	1.888	0.052	0.082	0.082
3′$_{ax}$	34.15	7.63	1.893	0.048	0.088	0.088

[a] Change of occupation numbers for donor oxygen lone pair.

[b] $\Delta \sigma^*_{Br-}$ and $\Delta \sigma^*_{X-}$ denotes the change in occupation number of antibonding orbitals.

4. Conclusions

In this work, the role of anomeric effect on halogen bonding has been examined with MP2 and CCSD(T) levels of theory. The halogen bonding interactions have been studied with electron donor molecule i.e., tetrahydro-1,3-oxazine and interhalogen compounds like FBr, BrCl and BrI. The MP2/aug-cc-pVDZ and CCSD(T)/aug-cc-pVDZ calculations showed that the axial oxygen lone pair is more available for the interaction with halogen atom compared to the equatorial lone pair of oxygen of tetrahydro-1,3-oxazine. The energy difference between the axial and equatorial conformers with

tetrahydro-1,3-oxazine:IBr complex attains up to 4.60 kJ/mol. The molecular electrostatic isopotential surface analysis showed the presence of positive electrostatic potential region on the extension of X-R bond. The electron-withdrawing nature of substituents plays a role to increase the maximum positive electrostatic potential ($V_{s,max}$), which is further responsible for strengthening the halogen bonding. The AIM analysis shows the extra stabilization in axial halogen bonded complexes due to the presence of additional bond critical point, which is formed by hydrogen bonding between the interacting electronegative halogen atom and the axial substituted NH/CH hydrogen atom. The calculated localized molecular orbital energy decomposition analysis (LMO-EDA) shows that the stabilities of the O··Br and O··Cl halogen bonds are attributed mainly due to electrostatic and dispersion forces. The non-covalent interaction (NCI) index of the halogen bond has been analysed to visualize the noncovalent halogen bonding interactions in real space. The low-gradient isosurfaces with low densities indicates the stabilizing interactions of halogen bonding. The changes in electron density during the formation of the complexes are analysed by considering the electron density shifts in the complex structures. The NBO analysis also inferred that the considerable charge transfer takes place from the electron donor oxygen atom to the antibonding orbital of interhalogen bond and in axial interaction, there is significant increase in occupation number of σ^*_{Br} or σ^*_{X} anti bonding orbital than equatorial one. The calculated results show that the halogen bonding interactions are appreciable with anomeric systems and such stereoelectronic effect can possibly dictate such interactions in a more directional manner. The importance of anomeric effect in governing the directionality of halogen bonding can be useful in the area of supramolecular chemistry and development of new pharmaceutical compounds in biological chemistry.

Conflict of interest

The authors declare that there is no conflict of interest.

Acknowledgments

Appendix A. Supplementary data:

Cartesian coordinates of all the geometries, including electronic energies are given in the supplementary data.

Highlights

❖ The role of anomeric effect on halogen bonding has been examined.

❖ Tetrahydro-1,3-oxazine and FBr, BrCl and BrI have been considered in this study.

❖ The axial oxygen lone pair is more available for the interaction with halogen atom.

❖ The role of substituents attached with the halogen atoms has also been evaluated.

References

1   A. J. Stone, Intermolecular Potentials, Science 321(2008) 787-789.

2   (a) I. Alkorta,F.Blanco, P. M.Deyà,J.Elguero,C.Estarellas,A.Frontera, D. Quiñonero,Cooperativity in multiple unusual weak bonds, Theor. Chem. Acc.126(2009) 1-14; (b) P.Deepa, B. V.Pandiyan,P.Kolandaivel, P.Hobza, Halogen bonds in crystal TTF derivatives: an *ab initio* quantum mechanical study, Phys. Chem. Chem. Phys. 16(2014) 2038-2047; (c) J.George, V. L.Deringer, R. Dronskowski, Cooperativity of Halogen, Chalcogen, and Pnictogen Bonds in Infinite Molecular Chains by Electronic Structure Theory, J. Phys. Chem. A118(2014) 3193−3200; (d) H. Ding, Y. Lu, W. Wu, H. Liu, Competing hydrogen bonding and halogen bonding interactions incrystal engineering: A case study of bi-functional donor molecules, Chemical Physics 441 (2014) 30–37.

3   P.Metrangolo,H.Neukirch,T.Pilati, G. Resnati, Halogen bonding based recognition processes: a world parallel to hydrogen bonding, Acc. Chem. Res.38(2005) 386-395.

4   (a) K. E.Riley,P.Hobza, On the importance and origin of aromatic interactions in chemistry and biodisciplines, Acc. Chem. Res.46(2013) 927-936; (b) X.Yang,L.Gan,L.Han,E.Wang, J. Wang, High-yield synthesis of silver nanoclusters protected by DNA monomers and DFT prediction of their photoluminescence properties, Angew. Chem., Int. Ed. Engl. 52(2013) 2022-2026; (c) J.Poznanski, D. Shugar, Halogen bonding at the ATP binding site of protein kinases: Preferred geometry and topology of ligand binding, Biochim.Biophys. Acta. 1834(2013) 1381-1386.

5   T. J.Mooibroek, P. Gamez, Halogen…phenyl supramolecular interactions in the solid state: hydrogen versus halogen bonding and directionality, Cryst Eng Comm. 15(2013) 1802-1805.

6   (a) L.Meazza, J. A.Foster,K.Fucke,P.Metrangolo,G.Resnati, J. W. Steed,Halogen-bonding-triggered supramolecular gel formation, Nat. Chem.5(2013) 42-47; (b) P.Metrangolo, F.Meyer,

T.Pilati, G.Resnati, G. Terraneo, Halogen bonding in supramolecular chemistry, Angew. Chem., Int. Ed. Engl. 47(2008) 6114-6127; (c) H. R.Khavasi, A. A. Tehrani, Influence of Halogen Bonding Interaction on Supramolecular Assembly of Coordination Compounds; Head-to-Tail N⋯X SynthonRepetitivity, Inorg. Chem.52(2013) 2891-2905.

7   (a) P.Politzer,P.Lane, M. C.Concha,Y.Ma, J. S. Murray,An overview of halogen bonding, J. Mol. Model.13(2007) 305-311; (b) P.Politzer, J. S.Murray, T. Clark, Halogen bonding: an electrostatically-driven highly directional noncovalent interaction, Phys. Chem. Chem. Phys. 12(2010) 7748-7757; (c) J. S.Murray, K. E.Riley, P.Politer, T. Clark, Directional Weak Intermolecular Interactions: σ-Hole Bonding, Aust. J. Chem. 63(2010)1598-1607; (d) P. Politzer, J. S. Murray, Halogen bonding: an interim discussion, ChemPhys Chem.14(2013) 278-294; (e) P.Deepa, R.Sedlak, P. Hobza, On the origin of the substantial stabilisation of the electron-donor 1,3-dithiole-2-thione-4-carboxyclic acid…I_2 and DABCO…I_2 complexes, Phys. Chem. Chem. Phys. 16(2014) 6679-6686; (f) R. Lo, A.Ballabh, A.Singh, P. Dastidar, B. Ganguly,Probing the O…Br–Br halogen bonding in X-ray crystal structures with *ab initio* calculations, CrystEngComm, 14(2012) 1833-1841; (g) A.Yu. Rogachev, R. Hoffmann, Iodine (I_2) as a Janus-Faced Ligand in Organometallics, J. Am. Chem. Soc. 135(2013) 3262−3275; (h) S. J. Grabowski, Halogen Bond and Its Counterparts: Bent's Rule Explains the Formation of Nonbonding Interactions, J. Phys. Chem. A 115(2011) 12340–12347.

8   K. E.Riley, K. M. Merz, Jr. Insights into the Strength and Origin of Halogen Bonding: The Halobenzene Bonding-Formaldehyde Dimer, J. Phys. Chem. A. 111(2007) 1688-1694.

9   P.Auffinger, F. A.Hays, E.Westhof, P. S. Ho, Halogen bonds in biological molecules, Proc. Natl. Acad. Sci. U. S.A. 101(2004) 16789-16794.

10   K. E.Riley, J. S.Murray, P.Politzer, M. C.Concha, P. Hobza, Br···O Complexes as Probes of
Factors Affecting Halogen Bonding: Interactions of Bromobenzenes and Bromopyrimidines with
Acetone, J. Chem. Theory Comput. 5(2009) 155–163.

11   R.Glaser, N.Chen, H.Wu, N.Knotts, M. Kaupp, ^{13}C NMR Study of Halogen Bonding of
Haloarenes: Measurements of Solvent Effects and Theoretical Analysis, J. Am. Chem.
Soc. 126(2004) 4412–4419.

12   C.Wang, F.Ying, W. Wu, Y. Mo, Sensing or No Sensing: Can the Anomeric Effect Be Probed by
a Sensing Molecule? J. Am. Chem. Soc.133(2011) 13731-13736.

13   (a) C. L.Perrin, K. B.Armstrong, M. A. Fabian, The origin of the anomeric effect: conformational
analysis of 2-methoxy-1,3-dimethylhexahydropyrimidine, J. Am. Chem. Soc.116(1994) 715-722;
(b) V. G. S. Box, The Role of Lone Pair Interactions in the Chemistry of the Monosaccharides.
The Anomeric Effects, Heterocycles 31(1990) 1157-1181; (c) V. G. S. Box, The anomeric effect
of monosaccharides and their derivatives. Insights from the new QVBMM molecular mechanics
force field, Heterocycles 48(1998) 2389-2417; (d) L. B.Favero, W.Caminati, B. Velino,
Conformation of dimethoxymethane: roles of anomeric effects and weak hydrogen bonds. A free
jet microwave study, Phys. Chem. Chem. Phys. 5(2003) 4776-4779; (e) A.Vila, R. A. Mosquera,
Atoms in molecules interpretation of the anomeric effect in the OCO unit, J. Comput. Chem.
28(2007) 1516-1530; (f) O.Takahashia, K.Yamasakia, Y.Kohnob, R.Ohtakib, K.Uedab,
H.Suezawac, Y.Umezawad, M. Nishioe,The anomeric effect revisited. A possible role of the CH/n
hydrogen bond, Carbohydr. Res. 342(2007) 1202-1209.

14   C. B. Anderson, D. T. Sepp, Conformation and the anomeric effect in 2-halotetrahydropyrans, J.
Org. Chem. 32(1967) 607-611.

15   (a) C. Møller, M. S. Plesset, Note on the Approximation Treatment for Many-Electron Systems,
Phys. Rev. 46(1934) 618; (b) T. H. Dunning, Gaussian Basis Sets for Use in Correlated Molecular

Calculations. I. The Atoms Boron through Neon and Hydrogen, J. Chem. Phys. 90(1989) 1007-1023; (c) D. E. Woon, T. H. Dunning, Gaussian basis sets for use in correlated molecular calculations. V. Core-valence sets for boron through neon, J. Chem. Phys. 103(1995) 4572-4585.

16   M. J. Frisch, G. W. Trucks, H. B. Schlegel, G. E. Scuseria, M. A.Robb, J. R. Cheeseman, G. Scalmani, V. Barone, B. Mennucci, G. A. Petersson, et al. Gaussian 09, Revision B01, Gaussian, Inc, Wallingford CT **2010**.

17   (a) S.Scheiner, Effects of Substituents upon the P⋯N Noncovalent Interaction: The Limits of Its Strength,J. Phys. Chem. A115(2011) 11202-11209; (b) U.Adhikari, S.Scheiner, Effects of Charge and Substituent on the S⋯N Chalcogen Bond,J. Phys. Chem.A118(2014) 3183-3192.

18   S. F. Boys, F.Bernardi, The calculation of small molecular interactions by the differences of separate total energies. Some procedures with reduced errors, Mol. Phys.19(1970) 553-566.

19   T. Lu, Multiwfn: A Multifunctional Wavefunction Analyzer, Version 3.0.1, Http://Multiwfn.Codeplex.Com, 2013.

20   P. Politzer, D. G.Truhlar, Chemical Applications of Atomic and Molecular Electrostatic Potentials; Plenum: New York, 1981.

21   W. Humphrey, A. Dalke, K. Schulten, Vmd: Visual Molecular Dynamics. J. Mol. Graphics., 14(1996) 33-38.

22   R.F. W.Bader, Atoms in Molecules: A Quantum Theory (Clarendon, Oxford, 1990).

23   F. Blieger-K nig, J. Sch nbohn, AIM2000, Version 2.0; chemical adviser, R. F. W.Bader, Büro fur Innovative Software StreibelBlieger- K nig: Germany, 2002.

24   NBO Version 3.1, E. D.Glendening, A. E.Reed, Eds.

25   (a) V. Dimitrova, S. Ilieva, B. Galabov, Electrostatic Potential at Atomic Sites as a Reactivity Descriptor for Hydrogen Bonding. Complexes of Monosubstituted Acetylenes and Ammonia, J. Phys. Chem. A 106(2002) 11801-11805; (b) O. Lukin, J. Leszczynski, Rationalizing the Strength

of Hydrogen-Bonded Complexes.Ab Initio HF and DFT Studies, J. Phys. Chem. A,106(2002) 6775-6782; (c) L. Joubert, P. L. A. Popelier, The prediction of energies and geometries of hydrogen bonded DNA base-pairs via a topological electrostatic potential, Phys. Chem. Chem. Phys.4(2002) 4353-4359; (d) J. S. Murray, P. Politzer, Electrostatic potentials of amine nitrogens as a measure of the total electron-attracting tendencies of substituents, Chem. Phys. Lett. 152(1988) 364-370; (e) M. Haeberlein, J. S. Murray, T.Brinck, P. Politzer, Calculated electrostatic potentials and local surface ionization energies of para-substituted anilines as measures of substituent effects, Can. J. Chem., 70(1992) 2209-2214.

26   V. V. Kuznetsov, Ab Initio conformational analysis of tetrahydro-1,3-oxazine, Russ. J. Org. Chem.46(2010) 117-120.

27   A. Bondi, van der Waals Volumes and Radii, J. Phys. Chem. 68(1964) 441-451.

28   (a) D.Vijay, H. Sakurai, V. Subramanian, G. N. Sastry, Where to bind in buckybowls? The dilemma of a metal ion, Phys. Chem. Chem. Phys.14(2012) 3057-3065; (b) N. Thellamurege, H. Hirao, Water Complexes of Cytochrome P450: Insights from Energy Decomposition Analysis, Molecules,18(2013) 6782-6791.

29   P.Su, H. Li, Energy decomposition analysis of covalent bonds and intermolecular interactions, J. Chem. Phys.131(2009) 014102-(1-15).

30   M. W. Schmidt, K. K. Baldridge, J. A. Boatz, S. T. Elbert, M. S. Gordon, J. H. Jensen, S. Koseki, N. Matsunaga, K. A. Nguyen, S. Su, et al. General atomic and molecular electronic structure system, J. Comput. Chem.14(1993) 1347-1363.

31   K. E. Riley,P.Hobza, Investigations into the Nature of Halogen Bonding Including Symmetry Adapted Perturbation Theory Analyses, J. Chem. Theory. Comput.,4(2008) 232-242.

32   L. Senthilkumar, T. K. Ghanty, S. K. Ghosh, Electron Density and Energy Decomposition Analysis in Hydrogen-Bonded Complexes of Azabenzenes with Water, Acetamide, and Thioacetamide, J. Phys. Chem. A 109 (2005) 7575-7582.

33   (a) S. J. Grabowski, E. Bilewicz,Cooperativity halogen bonding effect–Ab initio calculations on $H_2CO…(ClF)n$ complexes, Chemical Physics Letters 427(2006) 51–55; (b) S. J. Grabowski, QTAIM Characteristics of Halogen Bond and Related Interactions, J. Phys. Chem. A 116(2012) 1838−1845.

34   E. R. Johnson, S. Keinan, P. Mori-Sanchez, J. Contreras-Garcia, A. J. Cohen, W. Yang, Revealing Noncovalent Interactions, J. Am. Chem. Soc.132(2010) 6498-6506.

35   (a) J. Contreras-Garcia, E. R. Johnson, S. Keinan, R.Chaudret, J. P. Piquemal, D. N. Beratan, W. Yang, NCIPLOT: A Program for Plotting Noncovalent Interaction Regions, J. Chem. Theory Comput.7(2011) 625-632; (b) J. Contreras-Garcia, W. Yang, E. R. Johnson, Analysis of Hydrogen-Bond Interaction Potentials from the Electron Density: Integration of Noncovalent Interaction Regions, J. Phys. Chem. A115(2011) 12983-12990; (c) N. Han, Y. Zeng, X. Li, S. Zheng, L.Meng, Enhancing Effects of Electron-Withdrawing Groups and Metallic Ions on Halogen Bonding in the $YC_6F_4X···C_2H_8N_2$ (X = Cl, Br, I; Y = F, CN, NO_2, $LiNC^+$, $NaNC^+$) Complex, J. Phys. Chem. A 117(2013) 12959–12968.

36   H.Zhuo, H. Yu, Q. Li, W. Li, J. Cheng, Some measures for mediating the strengths of halogen bonds with the B–B bond in diborane (4) as an unconventional halogen acceptor,Int. J. Quant. Chem.114(2014) 128-137.

37   N. J. M.Amezaga, S. C. Pamies, N. M. Peruchena, G. L. Sosa, Halogen Bonding: A Study based on the Electronic Charge Density, J. Phys. Chem. A.114(2010) 552-562.